geosciences

MDPI

Article

Clay Minerals and Detrital Material in Paleocene–Eocene Biogenic Siliceous Rocks (Sw Western Siberia): Implications for Volcanic and Depositional Environment Record

Pavel Smirnov [1,2,*], Oksana Deryagina [1,3], Nadezhda Afanasieva [4], Maxim Rudmin [5] and Hans-Jürgen Gursky [2]

[1] Laboratory of Sedimentology and Paleobiosphere Evolution, University of Tyumen, Volodarskogo St. 6, 625003 Tyumen, Russia
[2] Institute of Geology and Paleontology, Clausthal University of Technology, Adolph-Roemer-Straße 2A, 38678 Clausthal-Zellerfeld, Germany; gursky@geologie.tu-clausthal.de
[3] Laboratory of Lithological and Petrophysical Studies of Rocks, West Siberian Geological Center, Surgutskaya St. 11/2, 625002 Tyumen, Russia; deriaginaoksanazsgc@yandex.ru
[4] Institute of Geology and Petroleum Technology, Kazan Federal University, Kremlevskaya St. 4/5, 420008 Kazan, Russia; n-afanasieva@rambler.ru
[5] Division for Geology, National Research Tomsk Polytechnic University, Lenina St. 30, 634050 Tomsk, Russia; rudminma@tpu.ru
* Correspondence: geolog.08@mail.ru; Tel.: +7-922-483-80-90

Received: 10 February 2020; Accepted: 27 April 2020; Published: 29 April 2020

Abstract: The paper presents the results of a study on clay minerals and detrital material of biosiliceous rocks (Paleocene–Eocene) from three sections in the Transuralian region. The authigenic processes in sediments resulted in the formation of dioctahedral clay minerals (illite, smectite) and insignificant amounts of sulfide phases (pyrite, hydrotroillite). Detrital minerals from the studied diatomites and diatomaceous clays often have a subangular and semi-rounded habit that is evidence of a low degree alteration of the sedimentary material in the provenance areas. The high degree of preservation of the bioclastic debris and the transformation of the limited volcanogenic substratum in clay minerals apparently was possible by initial burial diagenesis. The morphology of kaolinite and illite suggests that these mineral formations were caused by diagenesis with feldspars and smectites as a substrate for their formation. The smectite zone of weathering crust that developed on the adjacent land could have also served as a significant source of smectites entering the sea basin. The association with smectite in aggregates of mixed clayey composition indicates a sequential smectite-to-illite reaction via mixed-layered minerals. Such minerals as amphiboles, pyroxenes, and olivines, semi-stable to transportation and genetically associated with ultramafic rocks, form a significant part of the clastic fraction of the rock, indicating the proximity of provenance areas. This is the evident reason that the provenance areas made of mafic and ultramafic rocks played an essential role.

Keywords: siliceous rocks; diatomite; diatomaceous clays; Transuralian region; Western Siberia; PETM

1. Introduction

Biogenic siliceous rocks, such as diatomites and diatomaceous clays, are widespread in the Late Paleocene–Early Eocene sediments found at the western and northern margins of Western Siberia. Since their discovery in the 1930s, these deposits have been used in industrial production. Despite a significant volume of previous work devoted to biosiliceous rocks of the Transuralian region and Western Siberia [1–8], the mineralogical and geochemical features of the sediments under consideration have been insufficiently studied.

Currently, there is considerable interest in studying the mineralogical composition and geochemical features of biosiliceous rocks because of the association of these sediments with the important climatic event that occurred in the Cenozoic–Paleocene–Eocene Thermal Maximum (PETM) [9–14]. In terms of global geological processes, the PETM is considered to be a period of catastrophic warming of the climate at the Paleocene–Eocene boundary by an average of 4–8 °C, which lasted approximately 70–170 kyr [11]. An analysis of negative carbon-isotope excursions (CIEs), which are recorded in both marine and continental sediments, serves as a reliable analytical tool for identifying the PETM [11,12,14]. The PETM was accompanied by the transformation of oceanic and atmospheric circulation systems, as well as an increase in the bioproductivity of the neritic zone of the sea [15–19]. Moreover, this event greatly affected seawater acidification [20], the development of anoxia [21], the conditions and character of sedimentation, and the geochemical and mineral compositions of marine and oceanic sediments.

The biotic change features, biotic succession scale, and invasion of thermophylic flora and fauna into the Paleocene–Eocene basin of Western Siberia, where their limited distribution was previously recorded, have already been considered in a series of scientific articles [10,11,22–24]. The large-scale climatic fluctuations in the natural environment and the dynamics of geological processes must necessarily be reflected in the lithology of the rocks, and particularly the siliceous ones, that were formed during the Paleocene–Eocene time. The lithological features of the diatomites of Western Siberia, which formed at the Paleocene–Eocene boundary, are of considerable interest for the reconstruction of the paleogeographic conditions of the early stages of biogenic silica sedimentation in the Paleogene West Siberian basin. The influence of the PETM on the sedimentation in the eastern part of the ancient West Siberian Sea, which was characterized by another set of hydrological, tectonic, and sedimentation conditions [12], is reflected in the geochemistry and specific mineral authigenesis (pyrrhotite and greigite) of oolitic iron minerals [25]. Nevertheless, the detailed analysis and correlation of the processes in both parts of the unified West Siberian Sea provide an understanding of the sedimentation processes that occurred in the West Siberian region.

In sections of the Transuralian region, including some that were studied by the authors, markers facilitating the diagnosis of intervals associated with the PETM have not yet been encountered. Moreover, as recent geochemical studies have shown [26], these sections are geochemically weakly contrasting and characterized by a high degree of homogeneity. The Paleocene–Eocene sections in the western and north-western parts of Western Siberia are highly siliceous, which results in a deficit of carbonate phases observed in the sediments, and a substantial portion of international research is based on their study. In this regard, opportunities are being sought to carry out studies that will make it possible to more clearly and reliably determine the differences in siliceous strata due to global climatic changes in the Early Paleogene. The purpose of this work was to study the features and nature of the clay minerals and detrital material in Paleocene–Eocene biosiliceous rocks in the Transuralian region, along with the possible implications for the volcanic and depositional environment record.

2. Materials and Methods

2.1. Brief Stratigraphy Statement

The stratigraphic subdivisions of the siliceous rock sequence in the West Siberian Province were primarily based on the results of micropaleontological studies.

Within the western and northern margins of Western Siberia, siliceous rocks are attributed to the Paleocene Serov Formation and Eocene Irbit Formation. The Serov Formation is composed of opoka, clay opoka, and opoka-like clays. In the middle of the Transuralian region, including Talitsa, Kamyshlov, Irbit, and Shadrinsk, the Serov Formation is principally represented by pale grey and less often grey-to-dark-grey rocks; in the Tyumen area, it is represented by opoka with interlayers of dense aleuritic clays and clayey–silty diatomites.

The Irbit Formation is composed of diatomites, diatomaceous clays, and rarely tripoli-like and opoka-like clays. The bedding of the sequence is nearly flat; the rocks are not metamorphosed. In the most complete sequences of the Transuralian region, the formation is subdivided into two sub-formations: lower and upper. The lower Irbit sub-formation is mainly represented by diatomites, diatomaceous clay, and rarely tripoli and opoka-like clays, and sometimes includes interlayers of quartz and glauconite–quartz siltstones and sandstones. The Upper Irbit sub-formation (10–150 m thick) is represented by gray to greenish-gray diatomaceous and smectite clays, clayey diatomites, and diatomites.

2.2. Objects and Analytical Methods

This paper presents new data on clay and detrital mineral assemblage of diatomites and diatomaceous clays. We studied diatomites and diatomaceous clays from three large natural and man-made outcrops located at the western margin of the ancient Siberian Sea (Figure 1). These rocks successively compose the primary part of the Paleocene–Eocene siliceous sequence, and they were formed before (Paleocene diatomites of the Brusyana section) and after the PETM (Eocene diatomites of the Irbit deposit and Eocene diatomaceous clays of the Shadrinsk deposit). The age of the rocks being studied was reliably established based on the results of diatom analysis in the previous work [7].

X-ray diffraction (XRD) analyses were performed on 10 powder samples for every object studied, and the measurement results were averaged. For the Brusyana section and Irbit deposit, thin sections were used, and the corresponding data were obtained for a set of 12 fractions; for the Shadrinsk deposit, a set of 11 fractions was used. For these thin sections, the minimum and maximum figures were used in the numerators of the fractions, with the average value in the denominators. A total of more than 250 scanning electron microscopy (SEM) images were obtained for the bulk and pelitic fraction samples.

Laboratory studies, including grain size and XRD analyses, as well as lithological–petrographic studies of the samples under optical and scanning electron microscopes, were performed in the laboratory of the West Siberian Geological Center and Industrial University of Tyumen.

The grain size composition of the rocks in the range of 0.01–1.0 mm was determined by sieving. The sedimentation method was used to obtain preparations with different size fractions for further study. The sorting coefficient (particle size/grain composition) was determined by the method of P. Trask (1932).

Lithological–petrographic studies were performed for the following size fractions (mm): 0.1–0.4 and 0.1–0.01. The morphology of the clay mineral particles, along with their relationships with other minerals and microstructure, were studied using a JEOL JSM 6510A scanning electron microscope equipped with a hardware–software complex (Industrial University of Tyumen, Tyumen). The spatial resolution was up to 2.5 nm, the acceleration voltage was up to 20 kV, and the beam current was 1 mA. Overview and detailed images were obtained, which made it possible to observe microstructural features, such as the size, morphology of the structural elements, sharp crystal faces, degree of crystal trend disturbance, and presence of defects. Clay minerals nomenclature was done according to [27]. In the diagnosis of clay minerals, we relied on the statement that glauconite is micaceous minerals with up to 20% smectite interlayers. Due to that, in cases where we could not determine a high content of interlayer potassium, we described glauconite-like granular formations as mixed-layer formations.

The mineral composition was measured using a DRON-4 X-Ray diffractometer, with the further processing of the diffractograms using the GeoQuant program, which made it possible to remove

automatic recognition errors and spurious peaks. To provide greater detail for the data obtained, measurements were performed for air-dried samples. XRD parameters: angular range 2.75–69.75; shooting speed—4; exposure time—4 s. in increments of 0.05 °C. The XRD study of the rocks was additionally controlled by lithological–petrographic studies in thin sections using a Nikon eclipse LV100 Pol optical microscope.

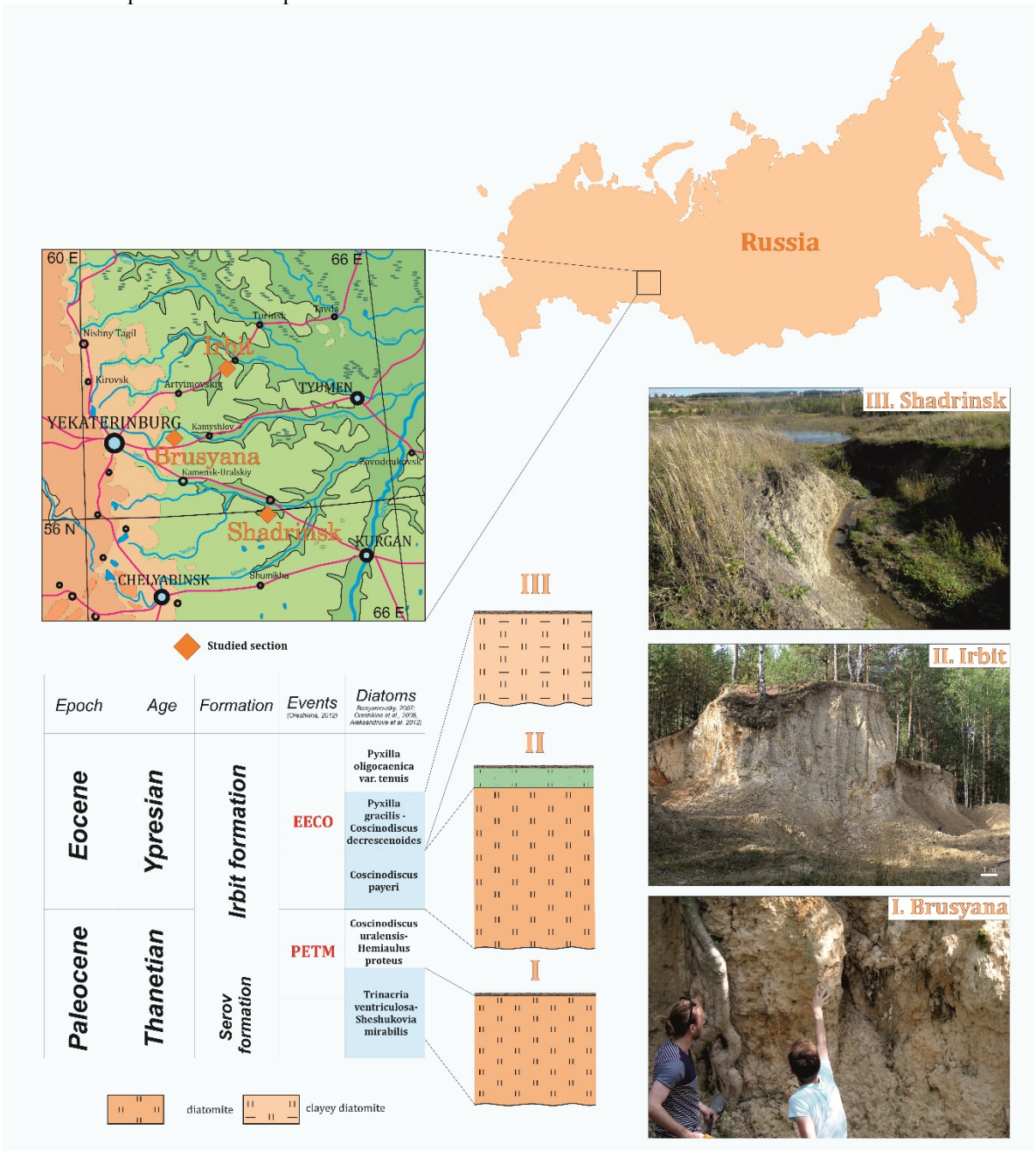

Figure 1. Location objects scheme and stratigraphic settings of the region. PETM—Paleocene–Eocene thermal maximum; EECO—Early Eocene Climatic Optimum.

3. Results

3.1. Lithological and Petrographic Features

The median particle sizes of all the rocks studied varied in a small range of 0.002–0.003 mm (Table 1). When the sorting coefficient So > 4.5, the rocks could be characterized as poorly sorted. The asymmetry coefficient Sk for rocks with different ages essentially varied, with Paleocene diatomites having values of 9.4–9.5, and Eocene diatomites and diatomaceous clays having values of 3.3–3.9. Accordingly, the

abundant introduction of coarse-grained material in the Paleocene diatomites of Brusyana was more pronounced. In any case, the speed of dynamic processing (sorting) of the detrital material exceeded the intensity of its influx for all studied objects.

3.1.1. XRD Data

The clay component was extremely diverse in composition. On the diffractograms of diatomites and diatomic clays, illite reflections with interplanar spacings of 9.9 Å, 10.00 Å, 5.0 Å, 4.47 Å, 2.57 Å were observed (Figure 2). The minerals of the smectite group were identified on the diffraction patterns of samples of Irbit, Brusyana and Shadrinsk. Smectites have labile interlayer spaces and, when air-dried, are characterized by basal reflections defined by the composition of the exchange cations. The interplanar distances of smectite reflections in the small-angle region for Irbit samples were 12.60 Å, Brusyana-14.63 Å, Shadrinsk-13.91 Å. Kaolinite was found in all samples of Brusyana, Irbit and Shadrinsk. It clearly stands out in the diffraction patterns according to the reflections of 7.20 Å and 3.58 Å.

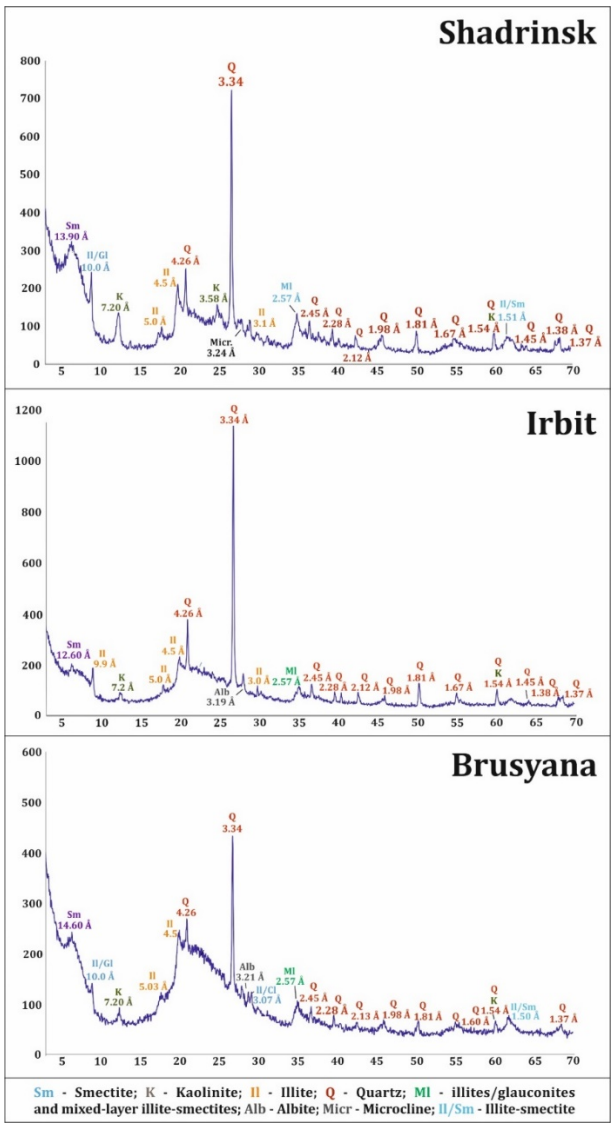

Figure 2. Representative X-ray diffraction (XRD) patterns of powder of air-dried samples.

Table 1. Results of grain size analysis.

Object	Psammitic Fraction							Aleuritic Fraction		Pelitic Fraction		
	Large		Medium			Small			Large	Small		
	1.0–0.8	0.8–0.5	0.5–0.4	0.4–0.25	0.25-0.2	0.2–0.16	0.16–0.1	0.1–0.05	0.05–0.01	0.01–0.005	0.005–0.001	<0.001
Shadrinsk	0.00	0.00	0.10	0.28	0.23	0.23	0.38	0.63	16.76	20.90	36.96	23.53
Irbit	0.00	0.00	0.03	0.33	0.30	0.38	0.98	2.15	21.05	23.20	33.47	18.11
Brusyana	0.00	0.10	0.05	0.25	0.20	0.34	1.35	7.35	14.19	19.19	40.59	16.39

3.1.2. Thin Sections

The data on the mineral distributions of the diatomites and diatomaceous clays in the compositions of fractions of 0.1–0.4 and 0.01–0.1 mm are presented in Table 2. The common feature for all the objects studied in thin-sections was the presence of mixed siliceous–clayey aggregates, composed of bioclastic debris (mainly diatom valves, both complete and fragments) and clayey minerals.

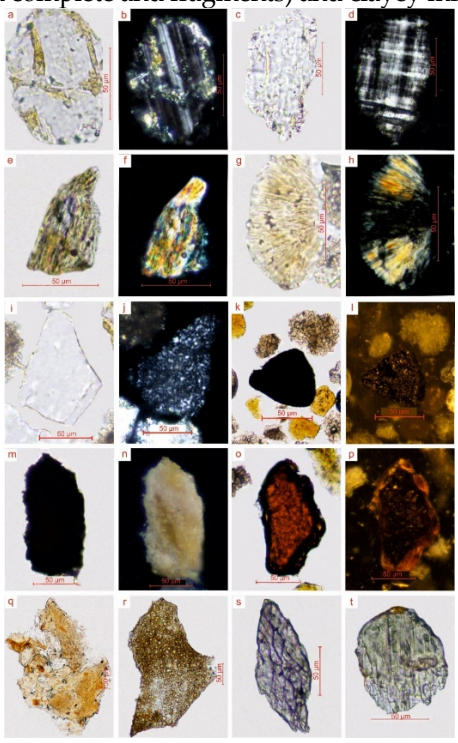

Figure 3. Minerals of the terrigenous fraction of diatomites and diatomaceous clays: Diatomites of the Irbit deposit: (**a–b**) plagioclase grain with fractures filled with illite: (**a**) parallel nicols, (**b**) crossed nicols; (**c–d**) a microcline grain with specific twin pattern: (**c**) parallel nicols, (**d**) crossed nicols; (**e–h**) hydrated flakes of biotite and muscovite, as well as a mica flake with authigenic quartz between fibers: (**e–g**) parallel nicols; (**f, h**) crossed nicols; (**i**) regenerated quartz grain, parallel nicols, (**j**) fragment of siliceous rock, crossed nicols; Diatomaceous clays of the Shadrinsk deposit: (**k,l**) rounded pyrite grain from fraction 0.01–0.1 mm: (**k**) parallel nicols; (**l**) in reflected light; (**m,n**) leucoxenized ilmenite grain: (**m**) parallel nicols; (**n**) in reflected light; Diatomites of the Brusyana section: (**o,p**) hematite: (**o**) parallel nicols; (**p**) crossed nicols; (**q–r**) volcanic glass fragments; glauconite with variable amount of small grains of ore minerals, in transmitted light; (**s**) amphibole; (**t**) rounded pyroxene grain, parallel nicols.

There were grains of quartz, feldspars, and rock fragments in the composition of diatomites and diatomaceous clays. Quartz grains were usually angular and semi-rounded, water-transparent, with point dusty inclusions, as well as regenerative borders up to 0.02 mm thick (Figure 3i). Feldspars were represented by acid plagioclases and microclines (Figure 3a,d). Secondary changes in feldspars were insignificant and were expressed in initial clay mineral formation. The presence of rounded plagioclase grains was noted for cracks filled with yellowish-green illite (Figure 3a,b). Rock fragments were mainly quartzite, micaceous and micaceous-quartz schists rock fragments were less common (Figure 3j). Acute-angled fragments of volcanic glass (Figure 3q,r), hornblende, and rounded pyroxene grains (Figure 3s,t) were also found in the diatomaceous clays and diatomites under consideration. The content of ore minerals was not significant, and did not exceed 1%–2% of the rock. Among which leukoxenized grains of ilmenite (Figure 3m,n), rounded grains of pyrite (Figure 4k,l), hematite (Figure 3o,p) were identified.

Mica/illite minerals were contained in the form of flakes; they formed continuous and discontinuous films around quartz grains and feldspars. Secondary changes in mica-like minerals were expressed in their kaolinite/chlorite formation (Figure 3g,h) and the release of authigenic quartz between fibers in swollen flakes (Figure 3e,f). Less commonly observed were plastically deformed and split at the ends of the plate. Fragments of volcanic glass and flakes of vermiculite-like minerals were diagnosed (Figure 4c,d). As a result of microscopic studies, fan-shaped mineral aggregates were identified, which were an alternation of packages of mica-like minerals and kaolinite. The presence of kaolinite was detected by the grayer interference colors in crossed nicols.

Table 2. The mineral composition of fractions of 0.1–0.4 and 0.01–0.01 mm, extracted from samples of diatomites and diatomaceous clays.

			Terrigenous Component, %				**Biogenic Component, %**								
Object	Fraction, mm	Content of a fraction in rock, %	Quartz	Feldspars	Fragments of rocks	Mica	Diatoms	Radiolarians and Silicoflagellates	Spicules of sponges	Siliceous--clayey aggregates	Sideritized aggregates	Mixed-layer illite–smectite clays	Epidote	Sphene	Ore minerals
S	0.1-0.4	1.1–4.7	1.8–2.8	-	-	-	2.1–6.7	1.5–4.4	-	86.8–94.2	-	-	-	-	-
	0.01–0.1	7.6–19.9	5.5–17.1	1.1–6.7	0.6–1.6	0.3–4.3	6.0–18.5	5.0–9.1	0.7–3.1	39.3–66.8	0.0–0.9	6.8–15.7	-	-	0.0–2.0
I	0.1–0.4	1.3–11.7	4.8–8.8	-	-	-	4.6–12.6	5.9–10.8	-	67.8–80.0	-	-	-	-	-
	0.01–0.1	10.9–28.2	13.3–26.9	7.6–17.3	0.7–1.9	0.4–1.6	10.2–20.3	1.0–3.3	2.1–6.2	20.9–42.3	1.7–5.5	3.9–12.2	0.0–0.8	0.0–0.5	0.7–1.7
B	0.1–0.4	2,.1–3.8	9.0–35.2	3.6–9.5	2.2–4.5	-	0.0–4.3	-	-	38.6–73.7	0.0–7.8	2.1–10.0	0.0–3.3	-	0.0–4.3
	0.01–0.1	7.1–21.5	22.9–29.6	4.8–15.7	1.3–4.6	1.3–4.4	1.6–6.2	0.0–2.7	0.9–1.7	18.5–44.0	0.6–5.6	12.3–20.5	0.9–4.0	0.0–1.5	0.9–4.3

S–Shadrinsk; I–Irbit; B–Brusyana.

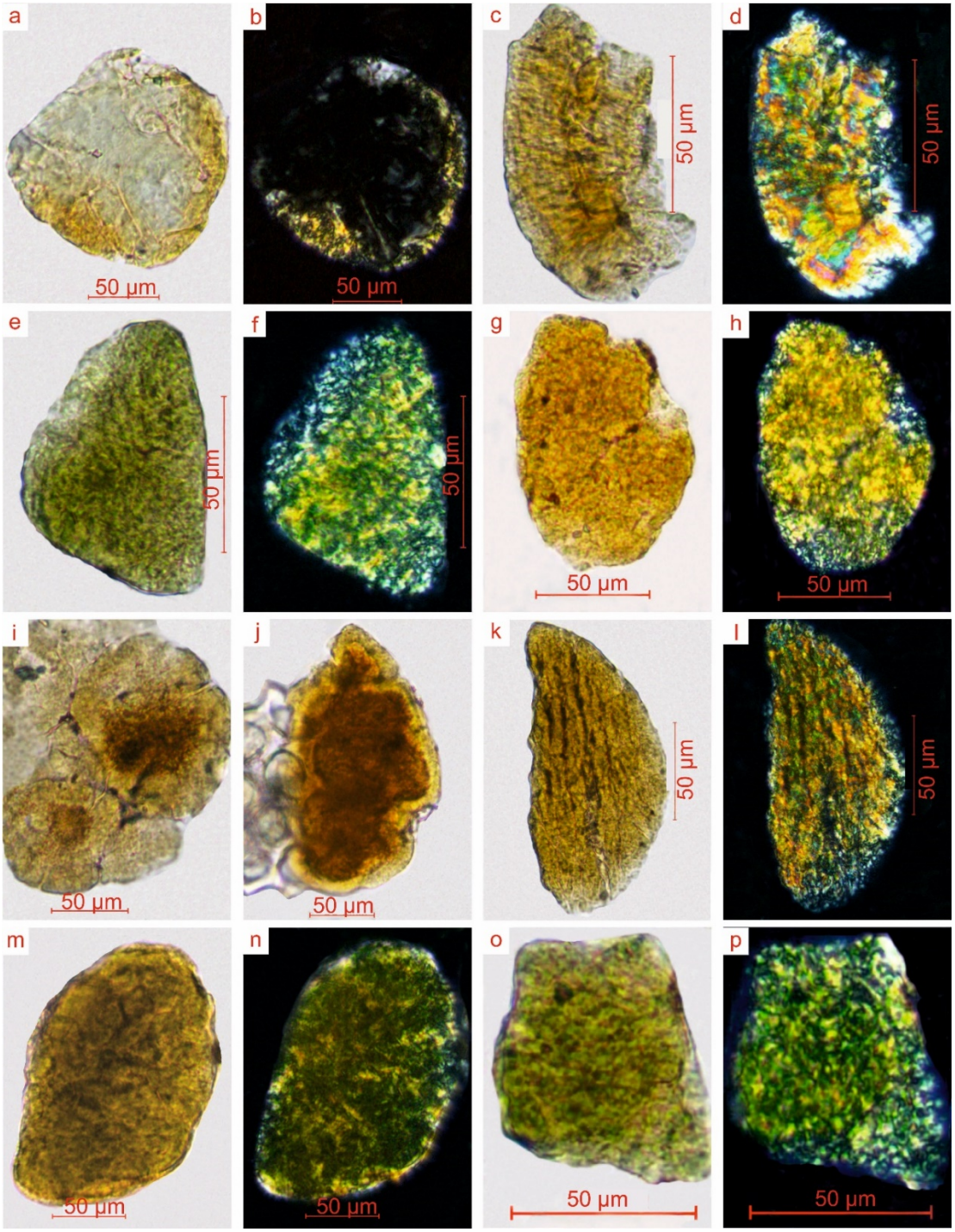

Figure 4. Mixed-layered illite–smectite formations in the rocks : (**a,b**) transformed volcanic glass fragment, rounded, with yellow rim (I morphotype): (**a**) parallel nicols; (**b**) crossed nicols; (**c,d**) lammelar-like highly inhomogeneous with high interreference colors (II morphotype); (**c**) parallel nicols; (**d**) crossed nicols; (**e,f**): semi-rounded yellow–green grains substrate on volcanic glass (III morphotype) (**e**) parallel nicols; (**f**) crossed nicols; (**g,h**) semi-rounded yellow grains (IV morphotype); (**g**) parallel nicols; (**h**) crossed nicols; (**i,j**) clay minerals formations with relics of biosiliceous substratum (V morphotype): (**i**) parallel nicols; (**j**) crossed nicols; (**k, l**) a volcanic glass fragment, sharply angular, with corrugated surface (VI morphotype): (**k**) parallel nicols; (**l**) crossed nicols; (**m,n**) highly rounded yellow grains substrate on volcanic glass (VII morphotype): (**m**) parallel nicols; (**n**) crossed nicols; (**o,p**) irregular shape green–yellow grains (VIII morphotype): (**o**) parallel nicols; (**p**) crossed nicols.

As in the case with the particle size distribution, obviously, a lower degree of sorting was observed in Brusyana diatomites. In the Eocene diatomites and diatomaceous clays, only siliceous

components (quartz, silica bioclastic, and mixed clay-siliceous aggregates) were actually present in the 0.1–0.4 mm fraction. There no such relationship existed in Samples Brusyana.

Newly formed glauconite-like grains of clay minerals of illite–smectite composition were yellowish-green, green, and greenish-yellow in color, with rounded and oval shapes; and not less than one-tenth of all the grains had syneresis fractures. Brownish grains with lighter rims contained iron hydroxides (Figure 4i–4g). Grains had a scaly and fiber-scaly structure. Some fragments of clay formations, which developed after the pyroclastics, had zoning: edge parts of the grains had been transformed into clay minerals of illite–smectite composition, while the rest of the grain preserved the ribbed structure of the primary pyroclastics (Figure 4i,j) or bioclastics (Figure 4k,l). Due to general mixed-layers illite–smectite and smectite with possible admixture of glauconites, that were separated based on thin sections analysis, we provide here several possible distinguishable morphotypes (Figure 4). There are – I: volcanic glass with a yellow rim of mixed-layered clay minerals; II: lammelar-like highly inhomogeneous with high interreference colors; III: semi-rounded yellow–green grains substrate on volcanic glass; IV: semi-rounded yellow grains; V: clay minerals formations with relics of biosiliceous substratum; VI: mixed-layers clay minerals formation on sharply angular volcanic glasses (with corrugated surface); VII: highly rounded yellow grains substrate on volcanic glass; VIII—irregular shape green–yellow grains

Apart from diatoms, the biogenic component contained single radiolarian shells, silicoflagellates, spicules of sponges, and mixed siliceous–clayey aggregates. Siliceous sponges were represented by thin, clean, transparent one-, three-, and four-axis spicules.

Diagenetic alterations in spicules, which are more stable than diatom valves, manifested silica minerals phase transitions. As a result, initially smooth spicules had a globular structure (Figure 5f), with the visible globules 3.5–9.1 μm in size. These globules were surrounded by thin outer rims of <1.0 to 1.5 μm in thickness. The signs of the recrystallisation of diatom valves into isotropic tridymite were recorded on the basis of the development of distinct newly formed faces on the diatom valve surfaces (Figure 6b–5c). Another example of diagenetic transformations of diatom valves and spicules of sponges associated with the phase transition was manifested in the occurrence of a well-defined shagreen surface, the disappearance of the net structure of the diatoms, and an axial channel for the spicules of sponges (Figure 6f).

Carbonate minerals (calcite and siderite) occurred in low concentrations and were identified in diatomites of the Irbit deposit and Brusyana section. Their proportion did not exceed 1%–2% of the bulk of the rock. Calcite rarely occurred as fragments. The content was a fraction of a percent. Siderite, as an admixture, was found in the composition of clayey–siliceous aggregates.

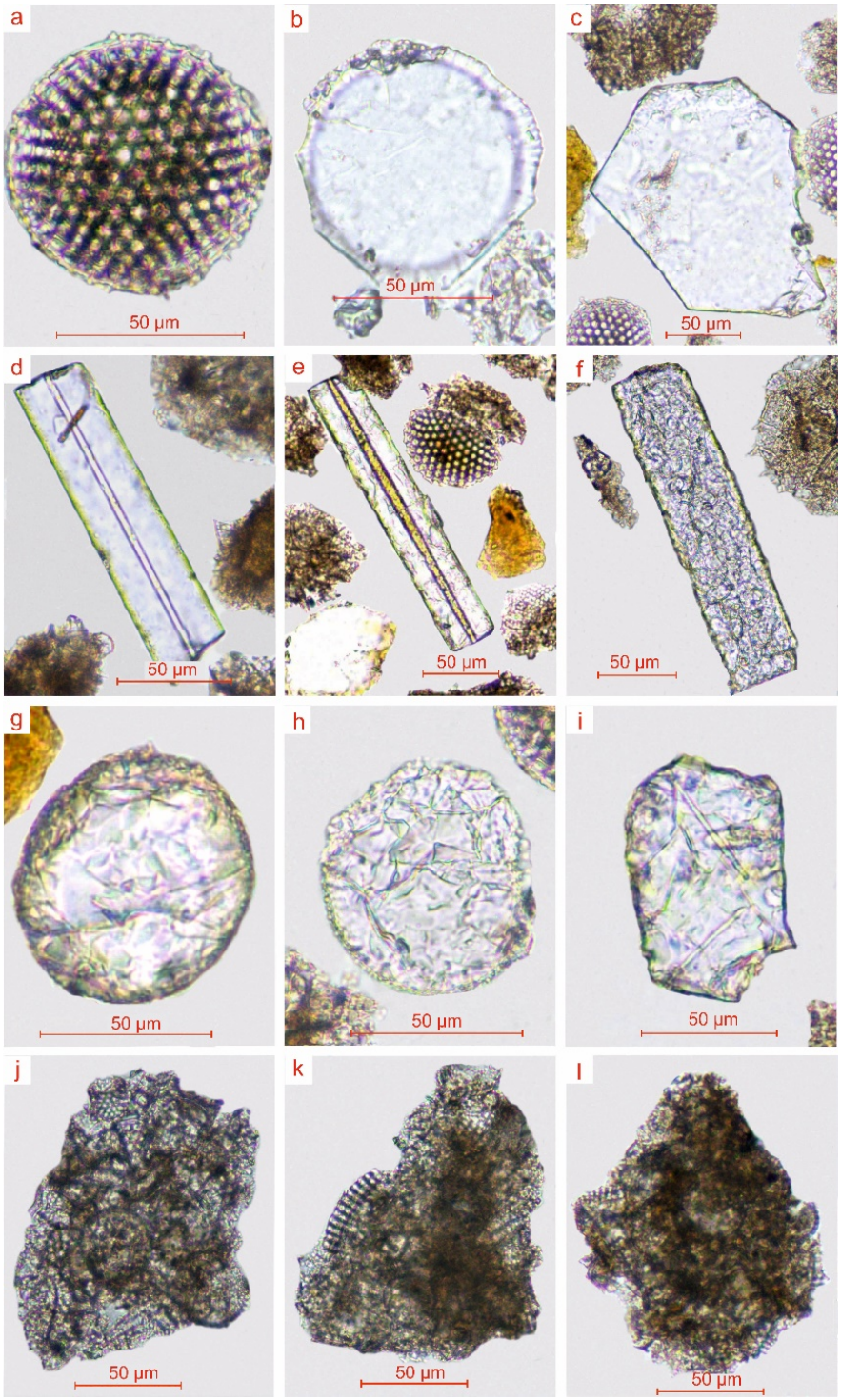

Figure 5. Biosiliceous components and the products of their transformation: Irbit deposit: (**a**) diatom valve; Shadrinsk deposit: (**b,a**) diatom valve recrystallized in tridymite, with newly-formed faces (fraction 0.01–0.1 mm); (**c**) tridymite crystal; (**d–f**) spicules of sponges: (**d**) sponge spicule in the axial channel, filled with a liquid; (**e**) sponge spicule with the axial channel, filled with Fe-rich illite; (**f**) spicule, altered and acquired globular structure; (**g–i**) fragments of sponge spicules, altered and morphologically different diatom detritus and grains of clayey minerals; (**j–l**) mixed clayey–siliceous aggregates.

3.2. *Structural and Morphological Features of Mineral Components*

Microscopical studies of the <0.01 mm fraction of the diatomites and diatomaceous clays revealed the similar sizes and morphologies of the mineral components (Figure 6).

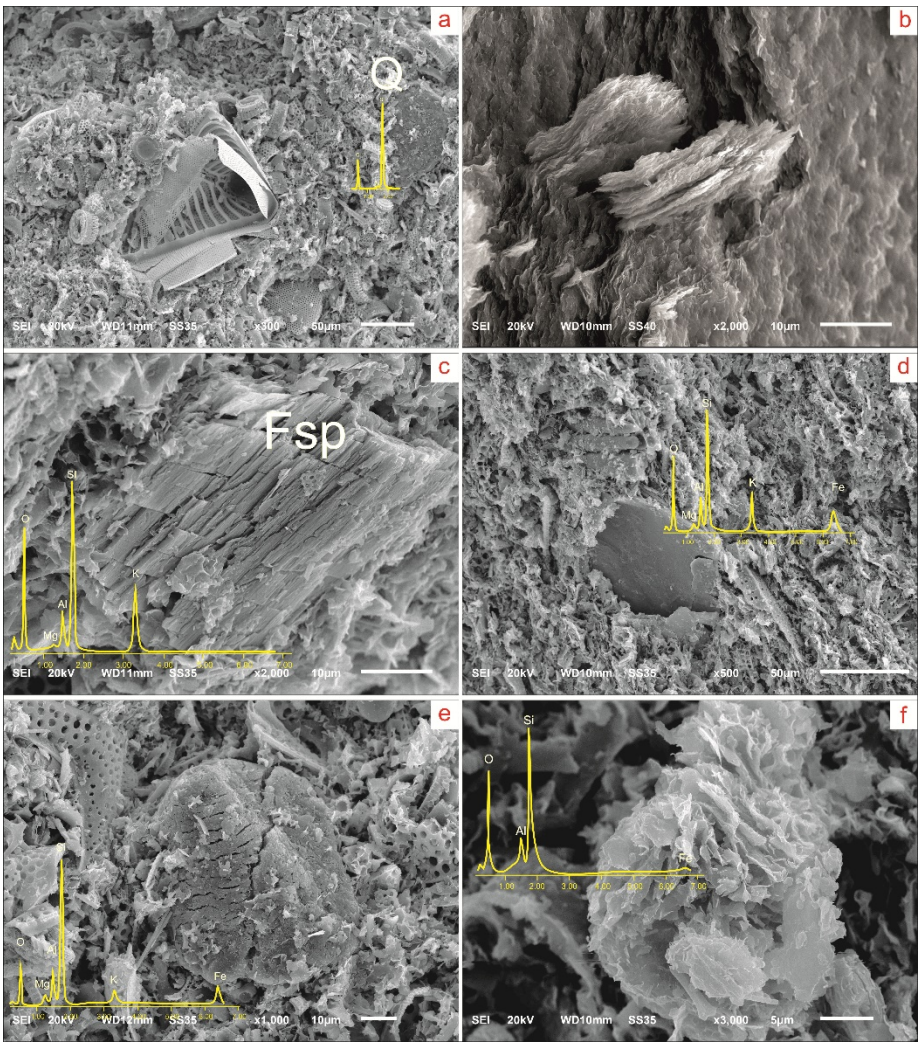

Figure 6. Scanning electron microscopy (SEM) images and Energy Dispersive X-Ray Spectroscopy (EDS) spectra of mineral components: (**a**) bioclastic debris and a single large quartz grain (Q); (**b**) illite, flake-shaped aggregates; (**c**) feldspar with traces of clay minerals formation (Fsp); (**d**,**e**,**f**) clay mineral formations: (**d**,**e**) illite or illite–smectite minerals; (**f**) kaolinite or kaolinite–smectite mixed-layer minerals

The study of the <0.01 mm fraction of the diatomites of the Brusyana section and Irbit deposit showed that nearly half of the field under consideration was represented by fine diatom detritus, frequent clayey–siliceous aggregates with easily recognizable diatom remains, and spicules of sponges. Fragments, which were similar to clay minerals in terms of their morphology, showed SiO_2 content in their spectra and belonged to quartz or bioclastic debris.

It was clearly seen under the microscope that the bulk (diatomaceous clays of the Shadrinsk deposit) contained flake-shaped aggregates, composed of smectite with single fibers and drop-like illite aggregates on the surface. Illite aggregates occurred rarely in association with other clayey minerals. Morphologically, they were fine flake-shaped aggregates made of subparallel small plates grown together. Such a morphology can indicate the detrital origin of the illite crystals.

Quartz grains varied in size, but were semi-rounded and subangular, with single well-crystallized grains. There were signs of the decomposition of feldspars (Figure 6c). Clays occurred as large flattened crystals (Figure 6d). The occurrence of dissected, eroded, and fragmentary faces of smectites or the presence of flake-shaped crystallites indicate the destruction and damage of grains during their transportation [28–30]. Authigenic smectite with a rose-like shape occurred, but it was less widespread. A small amount of sulfide phases (pyrite, hydrotroillite) was present in all the samples. The pyrite framboids

had different morphologies. The axial channels of sponges contained a new forming of illite–smectite mixed-layers clay minerals (Figure 7).

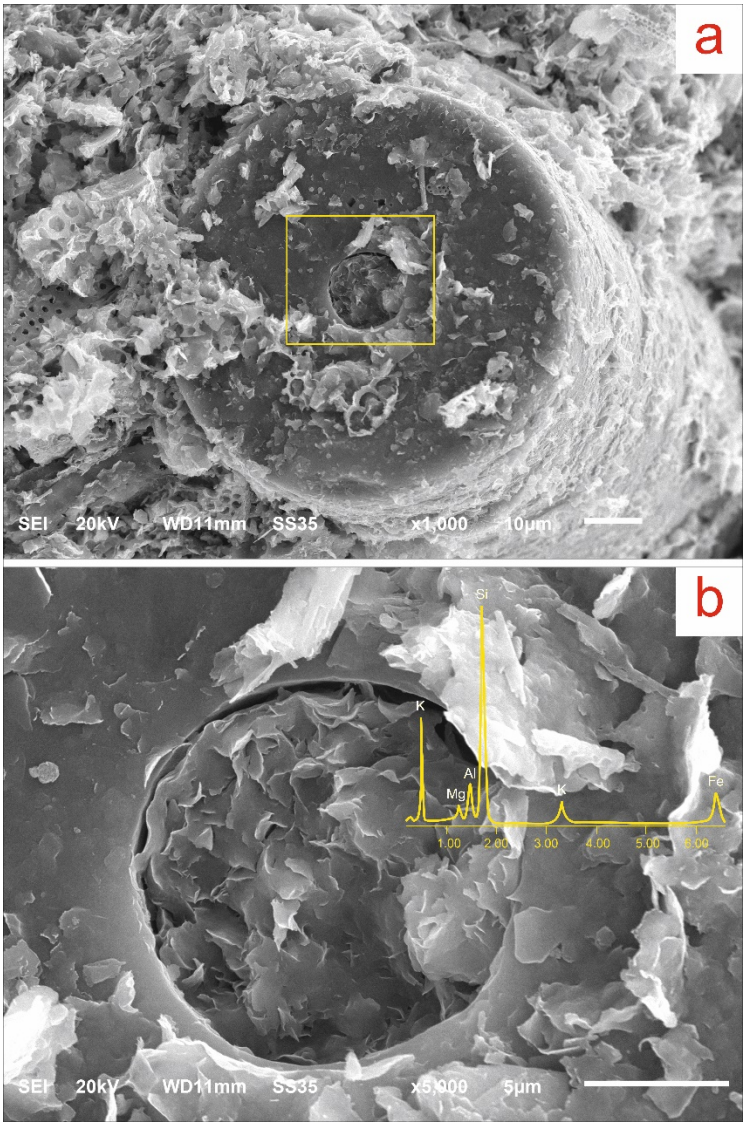

Figure 7. SEM images and EDS spectra of illite in the axis channel of a sponge spicule: (**a**) general view; (**b**) close-up view.

4. Discussion

Otherwise, the clay minerals and detrital material from objects of different ages did not have significant differences and, on the whole, testify to the similarity of conditions throughout the formation of the siliceous strata in the Paleocene and Eocene. In common data, it seems that quartz, feldspars, olivine, amphiboles, pyroxenes, part of kaolinite and illite are detrital, while Fe sulfides, smectites, part of illite and kaolinite are authigenic.

For clay minerals with a marine genesis, it is definitely possible to conclude that part of the smectite formed on a pyroclastic substrate. Secondary alterations of mica resulted in their hydration, new formations of kaolinite and chlorite and the development of authigenic quartz between fibers in swelling flakes.

The morphology of kaolinite and illite make the authors suggest that these minerals formation were caused by diagenesis with feldspars and smectites as a substrate for their formation. The association with smectite in aggregates of mixed clayey composition indicates a sequential smectite-to-illite reaction via mixed-layered minerals ("smectite illitization") in low-temperature environments and is commonly associated with a burial diagenesis [31–34]. We also consider the following statement relevant for the

studied rocks. Kaolinite is formed and stable in acidic environments, while smectite and illite tend to form under alkaline conditions [35–37]. Regarding that, it seems that the sedimentary process developed under weak alkaline conditions. In this case, a small amount of kaolinite among clay components proves its formation in later stages during diagenesis. In areas with a humid climate, the lower (smectite) zone of weathering crust that developed on the adjacent land could also have served as a significant source of smectites entering the sea basin.

In the rocks, transitional, mixed-layer forms of clay minerals are common. It becomes obvious that the formation of smectite along a volcanogenic substrate became widespread. Separate smectite particles inherited the morphological appearance of pyroclastic particles (Figure 4). The non-symmetric smectite reflex indicates absorbed complex composition inhomogeneity and the possible presence of mixed-layers clay minerals. Moreover, a large number of these smectites in diatomites occurred as smaller flakes; they were poorly crystallized and had a disordered structure. It seems reasonable to say that they belong to those of the Ge99 43 series , being similar in most of their parameters, according to XRD analyses. Smectites of this series are more highly charged and have more structural defects, indicating the unstable, rapidly changing conditions of their crystallization, which were probably due to post-volcanic hydrothermal activity. It has been established that ash pyroclastic material is the least stable solid phase of sediment, prone to various mineral transformations at all lithogenesis stages [38]. Its transformation during diagenetic transformations, which was recorded in microscopic studies, indicates that it is the main source of most of the smectite clays.

The studied diatomites contained smectites or illite–smectite of two different genetic types. The first type of swelling clay minerals was represented by greenish-yellow color flake (Figure 4c,d). These possibly have an evident terrigenous origin, and ancient weathering crusts can apparently be considered as their provenance areas. The second type of swelling clay minerals has an autigenic origin, and evidently predominates over the first type.

It is noteworthy that Paleocene diatomites of the Brusyana deposit were characterized by high contents of glauconite-like granular formations represented by illites/glauconites and mixed-layer illite–smectites. These minerals are dioctahedral micaceous phyllosilicate minerals with variable chemical composition and a high content of interlayer potassium (up to 4%–5%). Their internal structure revealed randomly distributed micro-flakes with jagged contours. We believe that the increase, albeit insignificant, in the amount of detrital material supplied from the land at the Paleocene–Eocene boundary was due to not only the detrital material supply as a result of continental weathering but also to a deep erosional trend and the capture of detrital material at the beginning of the corresponding transgressive cycle [39,40]. Amphiboles, pyroxenes, and olivines were indicated are semi-stable during transportation, genetically related to the ultramafic rocks. That is a sign of proximity of the provenance areas. In general, detrital minerals in diatomites and diatomaceous clays were subangular and semi-rounded, which is evidence of a low degree of alteration of the terrigenous material. The poor sorting and presence of both angular and subrounded grains are probably evidence that several provenance areas existed (two at a minimum), each of which supplied the sedimentation basin with mineral components with different degrees of weathering and had a specific spectrum of structural, textural, and geochemical features.

In the modern era, the formation of ferruginous smectite at the bottom of the seas from an amorphous siliceous ferric gel in areas subjected to the discharge of hydrotherms has been established. Tsekhovsky [41] noted that at discharge sites, thermal waters have a detrimental effect on the microflora, and nutrient rocks accumulate only when moving away from the sources of hydrothermal discharge or in a period of weakening of their activity. For this reason, the participation of a hydrothermal source must be indirect.

The authigenic nature of clay formation is most clearly expressed by the example of the transformation of a volcanic substrate. Hydration, hydrolysis, and ion exchange reactions under hydrothermal processes lead to the alkalization of pore solutions and their saturation with cations, as well as the formation of thin clay films of smectite and illite [42] on the surface of clay material debris (Figure 4).

The issue of the transportation of the pyroclastic material into the sedimentation basin is of interest. On platform land in Central Eurasia, rare scattered foci of predominantly basalt volcanism [42] existed. The presence of isolated local volcanoes has been confirmed by effusive findings: in the Northern Aral Sea

region, at the northern border of the Kazakh shield, within the Minusinsk depression, and to the south-east of the Voronezh anteclise. The established acid composition of pyroclasts, along with their small dimensions and often acute angular particle morphology, may be evidence for enriching sediments with eolian ash material as a result of air transport from the west and North Atlantic (Figure 8). The Eocene time in the Northern Sea (North Atlantic igneous province (NAIP)) was characterized by the colossal formation of igneous mafic rocks during the continental break-up between Europe and Greenland [43–45].

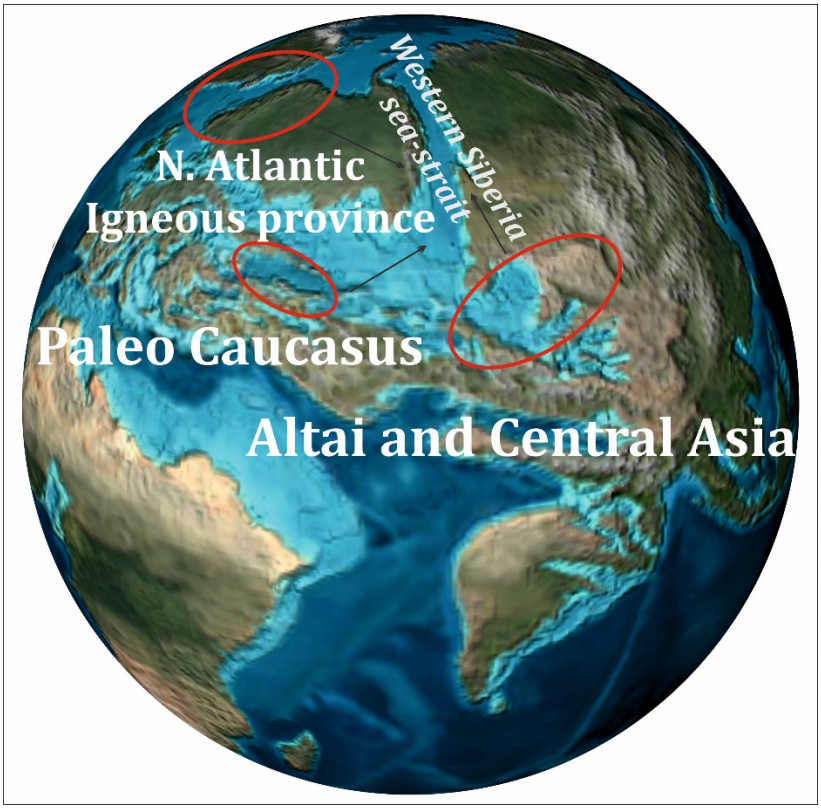

Figure 8. Eocene Northern Hemisphere configuration. NAIP—North Atlantic igneous province (as a possible pyroclastic material source).

At that time, a non-remote location in the North Atlantic igneous province provided the direct supply of the pyroclastic material in the sedimentary basin. Later, as the NAIP expanded and tectonic movements pushed these areas apart, the opportunities for pyroclastic material to access this basin became more limited.

It is evident that because of the remoteness, this process did not have any direct influence on silica accumulation in Western Siberia, and if the supply from the Northern Sea basin can only be assumed, it was rather indirect. Moreover, in connection with the felsic composition of the pyroclastics and, often, the angular morphology of the particles, it is hardly appropriate to talk about the leading role of the marine transportation of volcanic material. There are more signs that some portion of the pyroclastics was supplied to the West Siberian basin from ash clouds. As previously suggested, the sources of detrital material genetically associated with mafic and ultramafic rocks were localized in the proximity of the sedimentation basin.

The calculated lithochemical modules [26] indicate that the biogenic silica accumulation proceeded with a relatively high role played by chemical weathering on the adjacent land, which provided an additional transfer of the siliceous substance in the form of true or colloidal solutions to the sedimentation basin [26]. This proves that the relief of the land surrounding the Paleocene sea basin appears to have been comparatively unified and did not provide a significant amount of detrital material. The sandy material with a quartz–glauconite composition accumulated at the initial stage of the development of the Thanetian transgression. The Late Paleocene time was characterized by the distinct weakening of the activity of

tectonic movements in the adjoining land area. The main provenance areas were at the level of low denudation plains.

5. Conclusions

1. Authigenesis processes were involved in the formation of dioctahedral clay minerals (illite, smectite) and a small amount of sulfide phases (pyrite, hydrotroillite) in the formation. The morphology of kaolinite and illite suggests that these minerals' formation was caused by diagenesis with feldspars and smectites as a substrate for their formation. The association with smectite in aggregates of mixed clayey composition indicates a sequential smectite-to-illite reaction via mixed-layered minerals.

2. Clay minerals and detrital material from uneven-aged objects did not have striking differences, which, in general, indicates the similarity of conditions throughout the formation of the siliceous strata in the Paleocene and Eocene. For most clay minerals, it is definitely possible to conclude that part of smectite formed on a pyroclastic substrate primary volcanic glass structure preservation in some particles.

3. There was no significant difference in the characteristics of minerals with an authigenesis origin, and those of the associations in Paleocene and Eocene diatomites were established. In the Brusyana Paleocene diatomites, the content of psammitic detrital material may be a result of activation reasoned by the onset of the transgressive cycle, as well as simply the proximity to the coastline.

4. These biogenic siliceous rocks showed a small degree of modification of the detrital material, probably because of the proximity of the source of influx and the fact that the amount of detrital material was very limited. The observed small pyroclastic relics with an acute-angled form are assumed to be associated with the NAIP. There were several sources of detrital material: the first one of ultramafic composition was close to the sedimentation. The redeposited material with an acidic composition was of lesser significance and, apparently, further from the resedimention place.

Author Contributions: P.S. performed the fieldwork and sampling, as well as prepared all illustrations, funding acquisition and original draft preparation, P.S. and O.D. did the mineralogical analysis and microscopic studies. N.A., M.R., and H-J.G. participated in the conceptualization of the research and the discussion of the obtained data. All authors have read and agreed to the published version of the manuscript.

Funding: The reported study was funded by the Russian Foundation for Basic Research, project number 19-35-60004 «Sedimentology and geochemistry of marine siliceous formations of Western Siberia in the context of catastrophic thermal events of the Paleocene and Eocene».

Acknowledgments: We are grateful to Stig A. Schack Pedersen for the valuable advice and recommendations during our investigation. We thank Dmitriy V. Voroshchuk for translating an early version of the manuscript from Russian to English. We would like to thank the two anonymous reviewers for their constructive comments that improved the manuscript.

Conflicts of Interest: The authors declare no conflict of interest. The funders had no role in the design of the study; in the collection, analyses, or interpretation of data; in the writing of the manuscript, or in the decision to publish the results.

References

1. Distanov, U.G. *Siliceous Rocks of USSR*; Tatarskoe kn. izd: Kazan, Russia, 1976; 412 p.
2. Generalov, P.P.; Drozhashchikh, N.B. Eocene opalites of Western Siberia. In *Opalite of Western Siberia*; ZabSibNIGNI-Tyumen, Russia, 1987; pp 3–10. (In Russian).
3. Smirnov, P.V. Results of comprehensive studies of diatomite material composition from Irbit deposit. *Bull. Tomsk Polytech. Univ. Geo Assets Eng.* **2016**, *327*, 93–104.
4. Smirnov, P.V.; Konstantinov, A.O. Comparative studies of Eocene and Paleocene diatomite from Trans-Urals (on the example of Kamyshlov deposit and section Brusyana). *Bull. Tomsk Polytech. Univ. Geo Assets Eng.* **2016**, *327*, 96–102.

5. Smirnov, P.V. Preliminary results of revision of mineral-raw material base of opal-cristobalite rocks in middle Trans-Urals). *Bull. Tomsk Polytech. Univ. Geo Assets Eng.* **2017**, *328*, 28–37.
6. Smirnov, P.V.; Konstantinov, A.O. Diatomaceous Clay of Shadrinsky Deposit (Kurgan Region). *Georesursy = Georesources* **2016**, *18*, 240–244, doi:10.18599/grs.18.3.16.
7. Smirnov, P.V.; Konstantinov, A.O.; Gursky, H.-J. Petrology and industrial application of main diatomite deposits in the Transuralian region (Russian Federation). *Environ. Earth Sci.* **2017**, *76*, 682 doi 10.1007/s12665-017-7037-3.
8. Nesterov, I.I.; Smirnov, P.V.; Konstantinov, A.O.; Gursky, H.-J. Types, features, and resource potential of Palaeocene–Eocene siliceous rock deposits of the West Siberian Province: A review, *Int. Geol. Rev.* **2020**, doi:10.1080/00206814.2020.1719370.
9. Dunkley Jones, T.; Lunt, D.J.; Schmidt, D.N.; Ridgwell, A.; Sluijs, A.; Valdes, P.J.; Maslin, M. Climate model and proxy data constraints on ocean warming across the Paleocene–Eocene Thermal Maximum. *Earth-Sci. Rev.* **2013**, *125*, 123–145 doi:10.1016/j.earscirev.2013.07.004.
10. Frieling, J.; Iakovleva, A.I.; Reichart, G.-J.; Aleksandrova, G.N.; Gnibidenko, Z.N.; Schouten, S.; Sluijs, A. Paleocene-Eocene warming and biotic response in the epicontinental West Siberian Sea. *Geology* **2014**, *42*, 767–770, doi:10.1130/G35724.1.
11. McInerney, F.A.; Wing, S.L. The Paleocene–Eocene Thermal Maximum: A perturbation of carbon cycle, climate, and biosphere with implications for the future. *Annu. Rev. Earth PL Sc.* **2011**, *39*, 489–516, doi:10.1146/annurev-earth-040610-133431.
12. Smirnov, P.V.; Konstantinov, A.O. Biogenic siliceous accumulation in Early Paleogene marine basins of Western Siberia: Factors and stages. *Litosfera* **2017**, *17*, 26–47 (In Russian).
13. Thomas, E.; Shackleton, N.J. The Paleocene-Eocene benthic foraminiferal extinction and stable isotope anomalies. *Geol. Soc. Spec. Publ.* **1996**, *101*, 401–441, doi:10.1144/GSL.SP.1996.101.01.20.
14. Zachos, J.C.; Wara, M.W.; Bohaty, S.; Delaney, M.L.; Petrizzo, M.R.; Brill, A.; Premoli-Silva, I. A transient rise in tropical sea surface temperature during the Paleocene-Eocene Thermal Maximum. *Science* **2003**, *302*, 1551–1554. 10.1126/science.1090110.
15. Kennett, J.P.; Stott, L.D. Abrupt deep-sea warming, paleoceanographic changes and benthic extinctions at the end of the Paleocene. *Nature* **1991**, *353*, 225–229.
16. Bains, S.; Norris, R.D.; Corfield, R.M.; Faul, K.L. Termination of global warmth at the Palaeocene/Eocene boundary through productivity feedback. *Nature* **2000**, *407*, 171–174, doi:10.1038/35025035.
17. Gavrilov, Y.O.; Shcherbinina, E.A.; Oberhänsli, H. Paleocene-Eocene boundary events in the Northeastern Peri-Tethys. *Geol. Soc. Am. Spec. Pap*. **2003**, *369*, 147–168, doi:10.1130/0-8137-2369-8.147.
18. Shcherbinina, E.; Gavrilov, Y.; Iakovleva, A.; Pokrovsky, B.; Golovanova, O.; Aleksandrova, G. Environmental dynamics during the Paleocene-Eocene thermal maximum (PETM) in the northeastern Peri-Tethys revealed by high-resolution micropalaeontological and geochemical studies of a Caucasian key section. *Palaeogeogr. Palaeoclimatol.* **2016**, *456*, 60–81, doi:10.1016/j.palaeo.2016.05.006.
19. Stassen, P.; Thomas, E.; Speijer, R.P. Paleocene-Eocene Thermal Maximum environmental change in the New Jersey Coastal Plain: Benthic foraminiferal biotic events. *Mar. Micropaleontol*. **2015**, *115*, 1–23, doi:10.1016/j.marmicro.2014.12.001.
20. Penman, D.E.; Hönisch, B.; Zeebe, R.E.; Thomas, E.; Zachos, J.C. Rapid and sustained surface ocean acidification during the Paleocene-Eocene Thermal Maximum. *Paleoceanography* **2014**, *29*, 357–369, doi:10.1002/2014PA002621.
21. Dickson, A.J.; Rees-Owen, R.L.; März, C.; Coe, A.L.; Cohen, A.S.; Pancost, R.D.; Shcherbinina, E. The spread of marine anoxia on the northern Tethys margin during the Paleocene-Eocene Thermal Maximum. *Paleoceanography* **2014**, *29*, 471–488, doi:10.1002/2014PA002629.
22. Iakovleva, A.I. Palynological reconstruction of the Eocene marine palaeoenvironments in south of Western Siberia *Acta Palaeobot.* **2011**, *51*, 229–248.
23. Oreshkina, T.V. Evidence of Late Paleocene–Early Eocene hyperthermal events in biosiliceous sediments of western Siberia and adjacent areas. *Austrian J Earth Sci*. **2012**, *105*, 145–153.
24. Oreshkina, T.V.; Oberhänsli, H. Diatom turnover in the Early Paleogene diatomite of the Sengiley section, middle Povolzhie, Russia: A response to the initial Eocene Thermal Maximum? *Geol. Soc. Am. Spec. Pap.* **2003**, *369*, 169–179, doi:10.1130/0-8137-2369-8.169.
25. Rudmin, M.; Roberts, A.P.; Horng, C.-S.; Mazurov, A.; Savinova, O.; Ruban, A.; Veklich, M. Ferrimagnetic iron sulfide formation and methane venting across the Paleocene-Eocene thermal maximum in shallow

marine sediments, ancient West Siberian Sea. *Geochem Geophy Geosy*. **2018**, *19*, 21–42, doi:10.1002/2017GC007208.

26. Smirnov, P.V.; Konstantinov, A.O.; Batalin, G.A.; Gareev, B.I. Variability in distribution of major and trace elements in Lower Eocene siliceous sections of Transuralian region (Russia). *Acta Geochim.* **2019**, *38*, 262–276, doi:10.1007/s11631-018-0290-7.
27. Guggenheim, S.; Adams, J.M.; Bain, D.C.; Bergaya, F.; Brigatti, M.F.; Drits, V.A.; Formoso, M.L.L.; Galan, E.; Kogure, T.; Stanjek, H. Summary of recommendations of nomenclature committees relevant to clay mineralogy: Report of the Association Internationale pour l'Etude des Argiles (AIPEA) Nomenclature Committee for 2006, *Clay Clay Miner.* **2007**, *55*, 761–772, doi:10.1346/CCMN.2006.0540610.
28. Arostegi, J.; Baceta, J.I.; Pujalte, V.; Carracedo, M. Late Cretaceous–Palaeocene midlatitude climates: Inferences from clay mineralogy of continental-coastal sequences (Tremp–Graus area, southern Pyrenees, N Spain). *Clay Miner.* **2011**, *46*, 105–126, doi:10.1180/claymin.2011.046.1.105.
29. Gao, Y.; Wang, C.; Liu, Z.; Zhao, B.; Zhang, X. Clay mineralogy of the middle Mingshui Formation (upper Campanian to lower Maastrichtian) from the SKIn borehole in the Songliao Basin, NE China: Implications for palaeoclimate and provenance. *Palaeogeogr. Palaeoclimatol.* **2013**, *385*, 162–170 doi:10.1016/j.palaeo.2012.10.038.
30. Wu, J.W.; Liu, Z.F.; Zhou, C. Late Quaternary glacial cycle and precessional period of clay mineral assemblages in the Western Pacific Warm Pool. *Chin. Sci. Bull.* **2012**, *57*, 3748–3760, doi:10.1007/s11434-012-5277-x.
31. Deconinck, J.F.; Strasser, A.; Debrabant, P. Formation of illitic minerals at surface temperatures in Purbeckian sediments (Lower Berriasian, Swiss and French Jura). *Clay Miner.* **1988**, *23*, 91–103.
32. Drits, V.A. Structural and chemical heterogeneity of layer silicates and clay minerals. *Clay Clay Miner.* **2003**, *38*, 403–432.
33. Lázaro, V.V. Illitization processes: Series of dioctahedral clays and mechanisms of formation. In *Diagenesis and Low-Temperature Metamorphism. Theory, Methods and Regional Aspects*; Nieto, F., Jiménez-Millán, J., Eds.; Seminarios SEM: Jaén, Spain, 2007; 3, pp. 31–39.
34. Tillick, D.A.; Peacor, D.R.; Mauk, J.L. Genesis of Dioctahedral Phyllosilicates during Hydrothermal Alteration of Volcanic Rocks: I. The Golden Cross Epithermal Ore Deposit, New Zealand. *Clay Clay Miner.* **2001**, *49*, 126–140. doi 10.1346/CCMN.2001.0490203.
35. Ryan, P.C.; Huertas, F.J. Reaction pathways of clay minerals in tropical soils: Insights from kaolinite-smectite synthesis experiments. *Clay Clay Miner.* **2013**, *61*, 303–318, doi:10.1346/CCMN.2013.0610410.
36. Beaufort, D.; Rigault, C.; Billon, S.; Billault, V.; Inoue, A.; Inoue, S.; Patrier, P. Chlorite and chloritization processes through mixed-layer mineral series in low-temperature geological systems—A review. *Clay Miner.* **2015**, *50*, 497–523, doi:10.1180/claymin.2015.050.4.06.
37. Du, J.; Cai, J.; Wang, G.; Zeng, X.; Bao, Y.; Liu, F. The effect of diagenetic environment on hydrocarbon generation based on diagenetic mineral assemblage in mudstone. *Petrol. Sci. Technol*. **2018**, *24*, 2132–2142, doi:10.1080/10916466.2018.1528274.
38. Brovkov, G.N. *Factors and Features Ash Pyroclastics Transformations//Volcanogenic-Sedimentary Lithogenesis. Brief Theses IV All-Union*; a seminar; Publishing House Dal-Nevostochnogo Polytechnic Institute: Yuzhno-Sakhalinsk, Russia, 1974; pp 37–39.
39. Akhmetiev, M.A.; Beniamovsky, V.N. The Paleocene and Eocene in the Russian part of West Eurasia. *Stratigr. Geo Correl*+ **2006**, *14*, 49–72, doi:10.1134/S0869593806010047.
40. Akhmetiev, M.A.; Zaporozhets, N.I.; Beniamovsky, V.N.; Aleksandrova, G.A.; Iakovleva, A.I.; Oreshkina, T.V. Open and semi-closed Paleogene marine systems in Northeastern Peri-Tethys: Stable and transitional biostratigraphic, paleogeographic and paleoclimatological aspects. *Austrian J. Earth Sci*. **2012**, *105*, 50–67.
41. Tsekhovsky, Y.G. Sedimentogenesis and geodynamics in the Cretaceous-Paleogene boundary at the epoch of continental peneplanation. Article 1. Central and Eastern Eurasia. *Litosfera* **2015**, *1*, 5–23.
42. Kirov, G.; Šamajova, E.; Nedialkov, R.; Stanimirova, T.S. Alteration processes and products of acid pyroclastic rocks in Bulgaria and Slovakia. *Clay Miner.* **2011**, *46*, 279–294, doi:10.1180/claymin.2011.046.2.279.
43. Eldholm, O.; Kjersti, G. North Atlantic volcanic margins: Dimensions and production rates. *J. Geophys. Res.-Atmos.* **1994**, *99*, 2955–2968, doi:10.1029/93JB02879.

44. Egger, H.; Brückl, E. Gigantic volcanic eruptions and climatic change in the early Eocene. *Int. J. Earth Sci*. **2006**, *95*, 1065–1070. doi 10.1007/s00531-006-0085-7.
45. Larsen, L.M.; Fitton, J.G.; Pedersen, A.K. Paleogene volcanic ash layers in the Danish Basin: Composition and source areas in the North Atlantic Igneous Province. *Lithos* **2003**, *71*, 47–80, doi:10.1016/j.lithos.2003.07.001.